

Published in final edited form as:

J Appl Biomech. 2013 October ; 29(5): 505–516.

Effects of age-related differences in femoral loading and bone mineral density on strains in the proximal femur during controlled walking

Dennis E. Anderson^{1,2} and Michael L. Madigan³

¹Center for Advanced Orthopaedic Studies, Beth Israel Deaconess Medical Center, Boston, MA, USA

²Department of Orthopedic Surgery, Harvard Medical School, Boston, MA, USA

³Department of Engineering Science and Mechanics, Virginia Polytechnic Institute and State University, Blacksburg, VA, USA

Abstract

Maintenance of healthy bone mineral density (BMD) is important for preventing fractures in older adults. Strains experienced by bone *in vivo* stimulate remodeling processes which can increase or decrease BMD. However, there has been little study of age differences in bone strains. This study examined the relative contributions of age-related differences in femoral loading and BMD to age-related differences in femoral strains during walking using gait analysis, static optimization, and finite element modeling. Strains in older adult models were similar or larger than in young adult models. Reduced BMD increased strains in a fairly uniform manner, while older adult loading increased strains in early stance but decreased strains in late stance. Peak ground reaction forces, hip joint contact forces, and hip flexor forces were lower in older adults in late stance phase, and this helped older adults maintain similar strains as young adults despite lower BMD. Because walking likely represents a “baseline” level of stimulus for bone remodeling processes, increased strains during walking in older adults might indicate the extent of age-related impairment in bone remodeling processes. Such a measure might be clinically useful if it could be accurately determined with age-appropriate patient-specific loading, geometry, and BMD.

Keywords

gait analysis; modeling; bone; kinetics; optimization

Introduction

Hip fractures are serious injuries that are associated with high rates of morbidity and mortality among older adults, and the incidence of hip fractures increases dramatically with age.¹ Because bone mineral density (BMD) accounts for about 70% of bone strength,² it is often used as a surrogate measure of bone strength and a predictor of fracture risk. Beginning at mid-life, BMD decreases with increasing age for both men and women.² Thus, age-related declines in BMD in part explain age-related increases in hip fractures, and the maintenance of BMD is important in preventing fractures among older adults.

Correspondence Address: Dennis E. Anderson, Center for Advanced Orthopaedic Studies, RN115, Beth Israel Deaconess Medical Center, 330 Brookline Ave, Boston, MA 02215, Phone: (617) 667-2940, Fax: (617) 667-7175, danders7@bidmc.harvard.edu.

Conflict of Interest Disclosure: The authors have no conflict of interest to disclose.

The loading experienced by a bone stimulates remodeling and adaptation, and can lead to the increase, maintenance, or loss of bone mass with increased, routine, or reduced loading, respectively.³ It has been reported that proximal femur BMD in young adults is associated with hip joint moments during walking, although this may⁴ or may not⁵ be independent of body mass. Strength training is associated with high BMD in both younger and older adults, and has a relatively site-specific effect⁶. Furthermore, femoral neck BMD is significantly correlated with hip abductor and flexor strength in postmenopausal women.^{7,8} Finite element modeling studies have been widely used to examine bone remodeling, for example following total hip replacement,⁹ with remodeling stimulus based on local strain energy density. However, there has been little examination of age-related differences in strains in the healthy intact femur, which may have implications for bone remodeling processes and maintenance of bone health in older adults.

Two factors that could affect strains in the femur, and thus remodeling stimulus, are femoral loading and femoral BMD, both of which may be subject to age-related differences. For example, older adults exhibit differences in gait kinetics compared to younger adults, including reduced ground reaction force (GRF),¹⁰ reduced hip flexion peak torque, power absorption, and negative work,^{11,12} and reduced plantar flexion peak torque, power generation, and positive work,¹¹⁻¹³ but increased hip extensor peak power generation and work.¹¹⁻¹³ Thus, there may be age-related differences in femoral loading during walking. In addition, due to the relationship between bone density and elastic modulus,¹⁴ older adults would tend to have lower femoral elastic modulus than young adults, which could increase femoral strains.

The purpose of this study was to examine the relative contributions of age-related differences in femoral loading during walking and age-related differences in femoral BMD to age-related differences in strains in the proximal femur. Muscle forces and hip joint contact forces during walking were estimated in young and older participants using gait analysis and static optimization and applied to finite element models of the femur. Strains in the proximal femur were calculated throughout the entire gait cycle in Young and Older models, as well as young models in which material properties were altered to match those of the older participants (Young-Old Materials) and young models in which the loading was altered to match the older participants (Young-Old Loads). We hypothesized that older adults would exhibit significantly lower peak ground reaction forces, hip joint forces, and muscle forces than young adults, except that older adults would have higher hip extensor forces. We further hypothesized that Older models would have larger peak strains and femoral head deflections than Young models, that Young-Old Materials models would have larger peak strains and femoral head deflections than Young models due to reduced elastic modulus, and that Young-Old Loads models would have smaller peak strains and femoral head deflections than Young models due to reduced loading.

Methods

Ten participants, including five young and five older adults, took part in gait testing, strength testing and dual energy x-ray absorptiometry (DXA) scans of the hip and entire femur performed using a GE Lunar Prodigy scanner (GE Healthcare, Chalfont St. Giles, UK). Participants reported having no musculoskeletal, neurological, cardiovascular, or cognitive disorders that might affect gait, and all could walk independently. The age groups were similar in that each contained two men and three women, and there were no statistically significant differences in height or body mass between groups (Table 1). This work was approved by the Virginia Tech Institutional Review Board, and the participants provided written informed consent prior to participation.

Gait testing consisted of participants walking down an 8 m walkway under controlled gait conditions. All participants walked with a controlled speed of 1.1 m/s and controlled step length of 0.65 m so that speed and step length were the same between age groups and would not affect age differences in femoral loading. These values fall within the range of speeds and step lengths reported in the literature for self-selected gait in older adults.^{10,12,13,15} GRF and body position data were collected over one full gait cycle of the right lower extremity. GRF data was sampled at 1000 Hz from a six degree-of-freedom force platform (Advanced Mechanical Technology Inc., Watertown, MA) placed in the center of the walkway. Thirty-six reflective markers were placed on each participant, and marker position data was sampled at 100 Hz using a six-camera VICON 460 motion analysis system (VICON Motion Systems Inc., Lake Forest, CA).

To estimate muscle forces, a subject-specific musculoskeletal model of the right lower limb was developed for each participant. These models were created in OpenSim, an open-source software system for musculoskeletal modeling,¹⁶ and based on a model of the legs and torso developed by Delp et al.¹⁷ Each model consisted of the pelvis, thigh, shank, and foot segments connected by hip, knee, and ankle joints. Subject-specific segment sizes were based on anthropometric measurements and the distances between joint centers, which were calculated by functional methods from marker position data.¹⁸ Subject-specific segment masses, center of mass positions, and mass moments of inertia were estimated from anthropometric data.^{19,20} All joints were modeled as three degree-of-freedom ball joints, but the knee and ankle were constrained to a single axis of rotation when calculating muscle forces. Thirty-five muscles of the lower extremity (Figure 1) were modeled as Hill-type musculotendon actuators.¹⁷

To create subject-specific muscle models, peak isometric muscle forces in the model were adjusted based on maximum isometric torque data collected using a Biodex System 3 dynamometer (Biodex Medical Systems, Inc., Shirley, New York, USA). Participants performed isometric maximum voluntary exertions for ankle plantar flexion, dorsiflexion, knee flexion, knee extension, and hip flexion, extension, abduction, and adduction at joint angles chosen to match the angles of maximum isometric joint torque.²¹ Baseline strengths of the muscles in the model were based on physiological cross-sectional area information taken from the literature.^{22,23} Corresponding maximum isometric torques were determined from the model, compared to experimental data, and the peak isometric muscle forces were adjusted iteratively. The process allowed for sufficient strength in the model such that the muscles could stabilize the hip joint while producing maximum torque about any particular axis.

Muscle forces were determined using static optimization, which has been widely used to estimate *in vivo* muscle forces during gait.^{24–28} This provides a method of distributing the required forces among the available muscles in order to solve the indeterminate problem of many muscles balancing the joint moments. In short, muscle forces are determined that meet an overall performance criterion at each time-point. The performance criterion used was minimizing the sum of muscle activation squared.^{24,25}

A finite element model of the femur was obtained from the public dataset of the VAKHUM project.²⁹ The model used was created from segmentation of a computed tomography scan and had material properties based on the computed tomography image, providing an approximation of material non-homogeneity in the femur. The model was available in six levels of mesh refinement, and a convergence test of these models was performed to select the model for use in this study. The selected model consisted of 17,696 linear hexahedral elements and had 217 linear elastic isotropic materials.

Subject-specific finite element models of the femur were created by adjusting the geometry and material properties of the VAKHUM femur model based on subject femoral geometry and areal BMD (aBMD) measured from the DXA scans. Femoral neck diameter, femoral neck axis length, and femoral length (from the top of the femoral head to the inter-condylar notch) were measured using the program ImageJ.³⁰ Subject-specific geometry was created by scaling the VAKHUM model based on each participant's femoral neck diameter, femoral neck axis length, femoral neck angle, and femoral length using a non-homogeneous scaling approach.³¹ The material densities in the VAKHUM model were adjusted so that they would match reasonable values for an older adult as described in the literature. Specifically, the femoral neck aBMD of the model was adjusted to be about 0.573 g/cm², average for a female over 80,³² and the densest material in the femoral neck was assigned an elastic modulus of 13.53 GPa, which is average for cortical bone at age 80,³³ and corresponds to a density of 1.579 g/cm³ based the equation of Morgan et al.¹⁴ Subject-specific model material densities were determined from the material densities in the adjusted VAKHUM model using the equation:

$$\rho_{SUBJECT} = \left(\frac{aBMD_{SUBJECT}}{d_{SUBJECT}} \cdot \frac{d_{VAKHUM}}{aBMD_{VAKHUM}} \right) \times \rho_{VAKHUM} \quad (\text{Eq. 1})$$

where ρ is a model material density, $aBMD$ is the aBMD of the femoral neck ($aBMD_{VAKHUM} = 0.573 \text{ g/cm}^2$), and d is the diameter of the femoral neck ($d_{VAKHUM} = 3.2 \text{ cm}$). Because aBMD is bone mineral content per projected area rather than volume, this equation includes femoral neck diameters to account for differences in bone size as well as aBMD when adjusting volumetric density. A range of 0.0 – 2.0 g/cm³ was considered reasonable for material densities in the models,³⁴ and material densities greater than this in subject-specific models were reduced to 2.0 g/cm³. The equation of Morgan et al.¹⁴ was used to convert material density to elastic modulus:

$$E = 6850\rho^{1.49} \quad (\text{Eq. 2})$$

where E is elastic modulus in MPa and ρ is apparent density in g/cm³. This relation provides excellent agreement between finite element results and *in vitro* strain measures in the femur under a variety of loading conditions.³⁴ Average element elastic modulus was 4.9 GPa (range 4.5 – 5.6 GPa) for the older adults and 6.3 GPa (range 5.6 – 7.4 GPa) for the young adults. Young and Older models were created with geometry, loading conditions, and material properties from young and older subjects, respectively. Young and older subjects were then paired by sex and body mass to create two groups of combined models. Young-Old Materials models had geometry and loading conditions from young subjects, but material properties from older subjects, and Young-Old Loads models had geometry and material properties from young subjects, but loading conditions from older subjects. A Poisson's ratio of 0.3 was used for all materials in all models.

Loads and boundary conditions were applied to the model to represent estimated femoral loading throughout a single gait cycle. Boundary conditions constrained the femur in all three translational degrees of freedom as well as axial rotation at the knee and in anterior-posterior and medial-lateral translation at the hip according to the recommendations of Spiers et al.³⁵ Hip contact force and boundary conditions were applied to a hemispherical part representing the acetabulum (Figure 2), which was connected to the femoral head via a surface-to-surface constraint. Muscle forces were applied for all muscle lines of action in the musculoskeletal model that attach directly to the femur except the gastrocnemius (see Figure 1). Muscle forces applied to the femur model were distributed across the eight surface nodes determined to be geometrically closest to the muscle attachment point in the musculoskeletal model. The resulting locations were qualitatively reasonable compared to published muscle

attachment data.³⁶ Loading was applied in a quasi-static manner at 1% increments of the gait cycle, and the model was solved using Abaqus (Dassault Systèmes Simulia Corp., Providence, RI, USA).

Loading results were compared between age groups, specifically GRFs, hip joint contact forces, hip extensor forces (gluteus maximus), hip flexor forces (iliopsoas), hip abductor forces (gluteus medius and minimus), and hip adductor forces (adductor magnus, longus, and brevis). From finite element models, femoral head displacement was determined as well as maximum principal, minimum principal, and maximum shear strains at element centroids in four elements around the circumference of the femoral neck (superior, anterior, inferior, and posterior) and four around the circumference of the sub-trochanteric femoral shaft (lateral, anterior, medial, and posterior)(Figure 2). Peaks in results variables in early and late stance were compared between Young and Older models using independent t-tests, while Young vs. Young-Old Materials and Young vs. Young-Old Loads comparisons were performed with paired t-tests. Significance was set at $\alpha=0.05$.

Results

Older adults did not have significantly different femoral size characteristics than young adults, but did have significantly lower femoral neck aBMD as measured by DXA (Table 1). Young and older adults walked at similar speeds of 1.18 ± 0.03 and 1.17 ± 0.05 m/s, respectively, and with similar step lengths of 0.65 ± 0.01 m in both age groups.

Mean force results throughout the gait cycle showed similar patterns in younger and older adults (Figure 3). Peak GRF, peak hip joint contact force, and peak hip flexor force in late stance were 9%, 18%, and 41% lower, respectively, in older adults compared to young adults (Table 2). No significant age differences were found in forces in early stance.

Maximum femoral head deflections averaged 2.4 ± 0.5 mm in Young and Older models, which is within a physiologically realistic range, in particular <4 mm.^{35,37} Peak femoral head deflections in early stance averaged 1.7 ± 0.2 mm in Young models, compared to 2.1 ± 0.5 mm in Older models ($P=.083$), 2.0 ± 0.3 mm in Young-Old Materials models ($P=.007$), and 1.9 ± 0.3 mm in Young-Old Loads models ($P=.132$ for two-tailed test). Peak femoral head deflections in late stance averaged 2.4 ± 0.3 mm in Young models, compared to 2.4 ± 0.8 mm in Older models ($P=.494$), 2.8 ± 0.4 mm in Young-Old Materials models ($P=.006$), and 2.1 ± 0.4 mm in Young-Old Loads models ($P=.190$). Mean maximum principal, minimum principal, and maximum shear strains for the femoral neck (Figure 4) and the sub-trochanteric region (Figure 5) followed similar trends as hip joint forces throughout the gait cycle. The largest peak maximum principal strains occurred in the superior femoral neck in late stance, while the largest minimum principal strains and maximum shear strains occurred in the posterior femoral neck in late stance for all models except the Young-Old Loads models, where they occurred in the inferior femoral neck (Table 3). All strains in the anterior femoral neck, posterior femoral neck, medial sub-trochanteric region, and posterior subtrochanteric region were larger in the Older models than the Young models in early stance, while in late stance minimum principal strains were larger in the anterior femoral neck. Strains in the Young-Old Materials models were uniformly larger than strains in the Young models. All strains in the posterior femoral neck, maximum principal strains in the anterior femoral neck, and minimum principal strains in the posterior sub-trochanteric region were smaller in the Young-Old Loads models than the Young models in late stance. However, maximum principal strain in the posterior sub-trochanteric region and minimum principal strain in the anterior sub-trochanteric region were larger in the Young-Old Loads models than the Young models in early stance.

Discussion

Mean peak strains in early stance phase averaged about 59% larger in Older models than Young models across all locations examined. At the same time, peak strains in the Young-Old Materials models averaged 43% larger than in the Young models, and peak strains in the Young-Old Loads models averaged about 12% larger than in the Young models. Note that this is contrary to the hypothesis that Young-Old Loads models would have smaller strains than Young models. However, peak hip extensor force was on average about 19% larger in older adults than in young adults, and although this difference did not reach significance ($P = .177$), it is consistent with known age-related differences in hip extensor peak power generation and work.¹¹⁻¹³ Thus, it appears that age-related differences in both femoral loading and BMD tend to increase strains in older adults compared to young adults in early stance, with the majority of the increase due to reduced BMD.

Mean peak strains in late stance phase averaged about 11% larger in Older models than Young models, across all locations examined, but this difference only reached significance in one location. At the same time, peak strains in the Young-Old Materials models averaged 44% larger than in the Young models, while peak strains in the Young-Old Loads models averaged about 17% smaller than in the Young models. As older adults exhibited lower femoral loading than younger adults in late stance, this is consistent with the hypothesis that age differences in femoral loading would decrease strains. It is worth noting that the largest strains, occurring in the superior and posterior femoral neck in late stance, were not significantly different between the Young and Older models. This suggests that reduced loading in older adults partially offsets the effect of reduced BMD, without which strains could be much higher as in the Young-Older Materials model. Increases in femoral neck cross-sectional area with age³⁸ could also help reduce strains in older adults, and older adults in this study did exhibit a trend toward 14% larger femoral neck diameter ($P = .099$). Thus, a combination of reduced loading and increased bone size may explain why femoral neck strains in the Older models were not much larger than the Young models in late stance despite lower BMD.

The hip joint contact forces found during gait were comparable in profile and magnitude to similarly determined forces in the literature.^{22,24,25,28,39} Similarly, the patterns and magnitudes of the muscle forces are consistent with previously reported muscle forces determined using static optimization.^{24,25,39,40} Static optimization predictions of hip joint forces correlate reasonably well overall with measurements from instrumented hip replacements²⁷ as well as with electromyography-based muscle force predictions.²⁶ It is worth noting that peak hip joint contact forces measured in hip replacement patients have been reported at around 250% of body weight,^{27,41} compared to a range of 400–500% of body weight reported in many static optimization studies of healthy subjects, including the current study.^{22,24,25,28,39} However, it is quite possible that hip replacement patients walk differently than healthy subjects which could result in reduced hip loading and largely explain this difference.

The femoral strains found in this study show similar patterns to previous finite element studies examining the femur during gait, with the medial femur in compression, and the lateral femur in tension in the sub-trochanteric region.^{35,37,42,43} The Young and Older models in this study appear to have similar strain magnitudes in the sub-trochanteric region as seen in previous finite element modeling studies.^{35,42} However, differences in material properties and loading conditions between this and previous studies make it unclear how directly comparable these results are, and data on femoral strains *in vivo* available for validation are very limited. Aamodt et al.⁴⁴ measured strains *in vivo* on the lateral proximal femur, and reported average principal tensile strains of about 1200 μ during the stance

phase of walking in one 49 year old woman. Comparable average values from this study are about 1500 μ for Young models and 1800 μ for Older models, which may indicate that strains estimated here exceed physiologic values somewhat. Additionally, some strain magnitudes seemed quite high for walking, for example in the femoral neck, where average peak compressive strains reached -4800 μ in older models. Thus, the strains determined in this study may be larger than femoral strains actually experienced during walking *in vivo*. While this does not negate the overall conclusions regarding the relative effects of age-related differences in BMD and femoral loading on strains, the absolute strain magnitudes should be interpreted with care. This also highlights the need for future studies to better quantify femoral strains *in vivo*.

This study employed both musculoskeletal and finite element modeling, and thus has many simplifications and limitations associated with it. For example, estimated muscle and joint reaction forces are affected by the optimization performance criterion used.^{25,40} The musculoskeletal model simplified lower extremity musculature to 43 muscle lines of action, ignoring other muscles and non-muscular structures that might produce loads. For example, loads produced by the ligaments of the hip joint capsule have been shown to change the stresses in the femoral neck.⁴⁵ Any errors in estimated loading would propagate to the finite element models. Muscle forces were applied to the femur model in locations representative of the musculoskeletal model rather than *in vivo* anatomy, and only muscles directly attaching to the femur were used. The finite element model for all subjects was created from a single existing model using scaling of geometry and material density. Geometric scaling could introduce element distortion, and scaling the material densities based on aBMD only allowed for gross adjustment of material properties. Specifically, individual or age-related differences in the distribution of material densities could not be accounted for, but could have a significant effect on femoral stiffness and strains. Finally, with a small sample size, power for statistical comparisons was quite limited. Nonetheless, this study includes all major muscle loads on the femur throughout the gait cycle, is the first to examine age differences in femoral strains during gait, and provides a reasonable first look at the relative effects of age-related differences in femoral loading and BMD on femoral strains.

Walking is a common source of femoral loading in both young and older adults, and a controlled speed and step length were used in order to produce similar gait in the two age groups. However, it is well established that older adults tend to walk with reduced speed and step length compared to young adults.¹⁵ Because GRFs and joint reaction forces increase with walking speed,²⁸ a similar analysis performed using self-selected gait would likely increase femoral loading, and hence strains, in young adults. However, this would not greatly alter the general findings of this study regarding the relative contributions of BMD and loading to age differences in strains. This study does not address possible age differences in loading during tasks besides walking, for example running, climbing stairs, or rising from a chair. The results of this study cannot be generalized to such very different tasks, and age-related differences in loading during such tasks could have very different effects on femoral strains.

In conclusion, this study indicates that older adults tend to have similar or larger femoral strains compared to young adults. Reduced BMD, as found in older adults, acts to increase strains, but the effect of age-related differences in loading is less consistent, tending to increase strains in early stance but reduce strains in late stance. The largest strains occurred in late stance, and without altered loading to help compensate for reduced BMD, strains might be very large in older adults. In healthy bone, large strains would act to stimulate remodeling processes and increase BMD. Unfortunately, the reason for reduced BMD in older adults is an imbalance in the bone remodeling process, with increased resorption and reduced formation due to decreasing number of osteoblasts and altered osteocyte activity.⁴⁶

On the other hand, bone remodeling can also take the form of periosteal apposition, which can increase bone size, such as femoral neck cross-sectional area,³⁸ with age. This would positively affect bone stiffness, and could help to reduce femoral strains in older adults. While strength training programs may help increase or maintain bone density in older adults, they tend to be most successful with high intensity exercises,⁶ presumably producing greater than “normal” strains. Loading above “normal” levels can stimulate remodeling in as few as 10–20 cycles per day.³ However, walking, as studied here, will generally accumulate many more cycles than this, and as such strains during walking likely represent a baseline or “normal” level of strain for bone remodeling processes. Thus increased strain during walking in older adults, as a measure of baseline remodeling stimulus, might be indicative of the extent to which bone remodeling processes are impaired. Such a measure might be clinically useful if it could be accurately determined, accounting for age-appropriate patient-specific loading, geometry (including periosteal apposition), and BMD.

Acknowledgments

We thank Dr. Robert West, Department of Mechanical Engineering, Virginia Tech, for technical advice and suggestions. Computational resources were provided courtesy of the Harvard School of Engineering and Applied Sciences and Dr. Robert Howe.

Funding: This work was supported by grants from the National Institute on Aging (F31AG030904; T32AG023480).

References

1. Melton LJ 3rd. Epidemiology of hip fractures: implications of the exponential increase with age. *Bone*. 1996; 18(3 Suppl):121S–125S. [PubMed: 8777076]
2. NIH. Osteoporosis prevention, diagnosis, and therapy. *JAMA*. 2001; 285(6):785–795. [PubMed: 11176917]
3. Turner CH. Three rules for bone adaptation to mechanical stimuli. *Bone*. 1998; 23(5):399–407. [PubMed: 9823445]
4. Moision KC, Hurwitz DE, Sumner DR. Dynamic loads are determinants of peak bone mass. *J Orthop Res*. 2004; 22(2):339–345. [PubMed: 15013094]
5. Bareither ML, Troy KL, Grabiner MD. Bone mineral density of the proximal femur is not related to dynamic joint loading during locomotion in young women. *Bone*. 2006; 38(1):125–129. [PubMed: 16112631]
6. Layne JE, Nelson ME. The effects of progressive resistance training on bone density: a review. *Med Sci Sports Exerc*. 1999; 31(1):25–30. [PubMed: 9927006]
7. Bayramoglu M, Sozay S, Karatas M, Kilinc S. Relationships between muscle strength and bone mineral density of three body regions in sedentary postmenopausal women. *Rheumatol Int*. 2005; 25(7):513–517. [PubMed: 16167163]
8. Zimmermann CL, Smidt GL, Brooks JS, et al. Relationship of extremity muscle torque and bone mineral density in postmenopausal women. *Phys Ther*. 1990; 70(5):302–309. [PubMed: 2333328]
9. Bitsakos C, Kerner J, Fisher I, Amis AA. The effect of muscle loading on the simulation of bone remodelling in the proximal femur. *J Biomech*. 2005; 38(1):133–139. [PubMed: 15519348]
10. Larish DD, Martin PE, Mungiole M. Characteristic patterns of gait in the healthy old. *Ann N Y Acad Sci*. 1988; 515:18–32. [PubMed: 3364884]
11. Monaco V, Rinaldi LA, Macri G, Micera S. During walking elders increase efforts at proximal joints and keep low kinetics at the ankle. *Clin Biomech (Bristol, Avon)*. 2009; 24(6):493–498.
12. Silder A, Heiderscheid B, Thelen DG. Active and passive contributions to joint kinetics during walking in older adults. *J Biomech*. 2008; 41(7):1520–1527. [PubMed: 18420214]
13. DeVita P, Hortobagyi T. Age causes a redistribution of joint torques and powers during gait. *J Appl Physiol*. 2000; 88(5):1804–1811. [PubMed: 10797145]

14. Morgan EF, Bayraktar HH, Keaveny TM. Trabecular bone modulus-density relationships depend on anatomic site. *J Biomech.* 2003; 36(7):897–904. [PubMed: 12757797]
15. Laufer Y. Effect of age on characteristics of forward and backward gait at preferred and accelerated walking speed. *J Gerontol A Biol Sci Med Sci.* 2005; 60(5):627–632. [PubMed: 15972616]
16. Delp SL, Anderson FC, Arnold AS, et al. OpenSim: open-source software to create and analyze dynamic simulations of movement. *IEEE Trans Biomed Eng.* 2007; 54(11):1940–1950. [PubMed: 18018689]
17. Delp SL, Loan JP, Hoy MG, et al. An interactive graphics-based model of the lower extremity to study orthopaedic surgical procedures. *IEEE Trans Biomed Eng.* 1990; 37(8):757–767. [PubMed: 2210784]
18. Piazza SJ, Erdemir A, Okita N, Cavanagh PR. Assessment of the functional method of hip joint center location subject to reduced range of hip motion. *J Biomech.* 2004; 37(3):349–356. [PubMed: 14757454]
19. de Leva P. Adjustments to Zatsiorsky-Seluyanov's segment inertia parameters. *J Biomech.* 1996; 29(9):1223–1230. [PubMed: 8872282]
20. Pavol MJ, Owings TM, Grabiner MD. Body segment inertial parameter estimation for the general population of older adults. *J Biomech.* 2002; 35(5):707–712. [PubMed: 11955511]
21. Anderson DE, Madigan ML, Nussbaum MA. Maximum voluntary joint torque as a function of joint angle and angular velocity: model development and application to the lower limb. *J Biomech.* 2007; 40(14):3105–3113. [PubMed: 17485097]
22. Brand RA, Pedersen DR, Friederich JA. The sensitivity of muscle force predictions to changes in physiologic cross-sectional area. *J Biomech.* 1986; 19(8):589–596. [PubMed: 3771581]
23. Klein Horsman MD, Koopman HF, van der Helm FC, et al. Morphological muscle and joint parameters for musculoskeletal modelling of the lower extremity. *Clin Biomech (Bristol, Avon).* 2007; 22(2):239–247.
24. Anderson FC, Pandy MG. Static and dynamic optimization solutions for gait are practically equivalent. *J Biomech.* 2001; 34(2):153–161. [PubMed: 11165278]
25. Glitsch U, Baumann W. The three-dimensional determination of internal loads in the lower extremity. *J Biomech.* 1997; 30(11–12):1123–1131. [PubMed: 9456380]
26. Heintz S, Gutierrez-Farewik EM. Static optimization of muscle forces during gait in comparison to EMG-to-force processing approach. *Gait Posture.* 2007; 26(2):279–288. [PubMed: 17071088]
27. Heller MO, Bergmann G, Deuretzbacher G, et al. Musculo-skeletal loading conditions at the hip during walking and stair climbing. *J Biomech.* 2001; 34(7):883–893. [PubMed: 11410172]
28. Rohrlé H, Scholten R, Sigolotto C, et al. Joint forces in the human pelvis-leg skeleton during walking. *J Biomech.* 1984; 17(6):409–424. [PubMed: 6480617]
29. Van Sint Jan, S. [Accessed 2008] The VAKHUM Project: Virtual Animation of the Kinematics of the Human for Industrial, Educational and Research Purposes. <http://www.ulb.be/project/vakhum/>
30. Abramoff MD, Magalhaes PJ, Ram SJ. Image processing with ImageJ. *Biophotonics International.* 2004; 11(7):36–42.
31. Lewis JL, Lew WD, Zimmerman JR. A nonhomogeneous anthropometric scaling method based on finite element principles. *J Biomech.* 1980; 13(10):815–824. [PubMed: 7462255]
32. Looker AC, Wahner HW, Dunn WL, et al. Updated data on proximal femur bone mineral levels of US adults. *Osteoporos Int.* 1998; 8(5):468–489. [PubMed: 9850356]
33. Zioupos P, Currey JD. Changes in the stiffness, strength, and toughness of human cortical bone with age. *Bone.* 1998; 22(1):57–66. [PubMed: 9437514]
34. Schileo E, Taddei F, Malandrino A, et al. Subject-specific finite element models can accurately predict strain levels in long bones. *J Biomech.* 2007; 40(13):2982–2989. [PubMed: 17434172]
35. Speirs AD, Heller MO, Duda GN, Taylor WR. Physiologically based boundary conditions in finite element modelling. *J Biomech.* 2007; 40(10):2318–2323. [PubMed: 17166504]
36. Viceconti M, Ansaloni M, Baleani M, Toni A. The muscle standardized femur: a step forward in the replication of numerical studies in biomechanics. *Proc Inst Mech Eng [H].* 2003; 217(2):105–110.

37. Taylor ME, Tanner KE, Freeman MA, Yettram AL. Stress and strain distribution within the intact femur: compression or bending? *Med Eng Phys.* 1996; 18(2):122–131. [PubMed: 8673318]
38. Riggs BL, Melton LJ 3rd, Robb RA, et al. Population-based study of age and sex differences in bone volumetric density, size, geometry, and structure at different skeletal sites. *J Bone Miner Res.* 2004; 19(12):1945–1954. [PubMed: 15537436]
39. Collins JJ. The redundant nature of locomotor optimization laws. *J Biomech.* 1995; 28(3):251–267. [PubMed: 7730385]
40. Monaco V, Coscia M, Micera S. Cost function tuning improves muscle force estimation computed by static optimization during walking. *Conf Proc IEEE Eng Med Biol Soc.* 2011; 2011:8263–8266. [PubMed: 22256261]
41. Bergmann G, Deuretzbacher G, Heller M, et al. Hip contact forces and gait patterns from routine activities. *J Biomech.* 2001; 34(7):859–871. [PubMed: 11410170]
42. Duda GN, Heller M, Albinger J, et al. Influence of muscle forces on femoral strain distribution. *J Biomech.* 1998; 31(9):841–846. [PubMed: 9802785]
43. Polgar K, Gill HS, Viceconti M, et al. Strain distribution within the human femur due to physiological and simplified loading: finite element analysis using the muscle standardized femur model. *Proc Inst Mech Eng [H].* 2003; 217(3):173–189.
44. Aamodt A, Lund-Larsen J, Eine J, et al. In vivo measurements show tensile axial strain in the proximal lateral aspect of the human femur. *J Orthop Res.* 1997; 15(6):927–931. [PubMed: 9497820]
45. Rudman KE, Aspden RM, Meakin JR. Compression or tension? The stress distribution in the proximal femur. *Biomed Eng Online.* 2006; 5:12. [PubMed: 16504005]
46. Dominguez LJ, Di Bella G, Belvedere M, Barbagallo M. Physiology of the aging bone and mechanisms of action of bisphosphonates. *Biogerontology.* 2011; 12(5):397–408. [PubMed: 21695491]

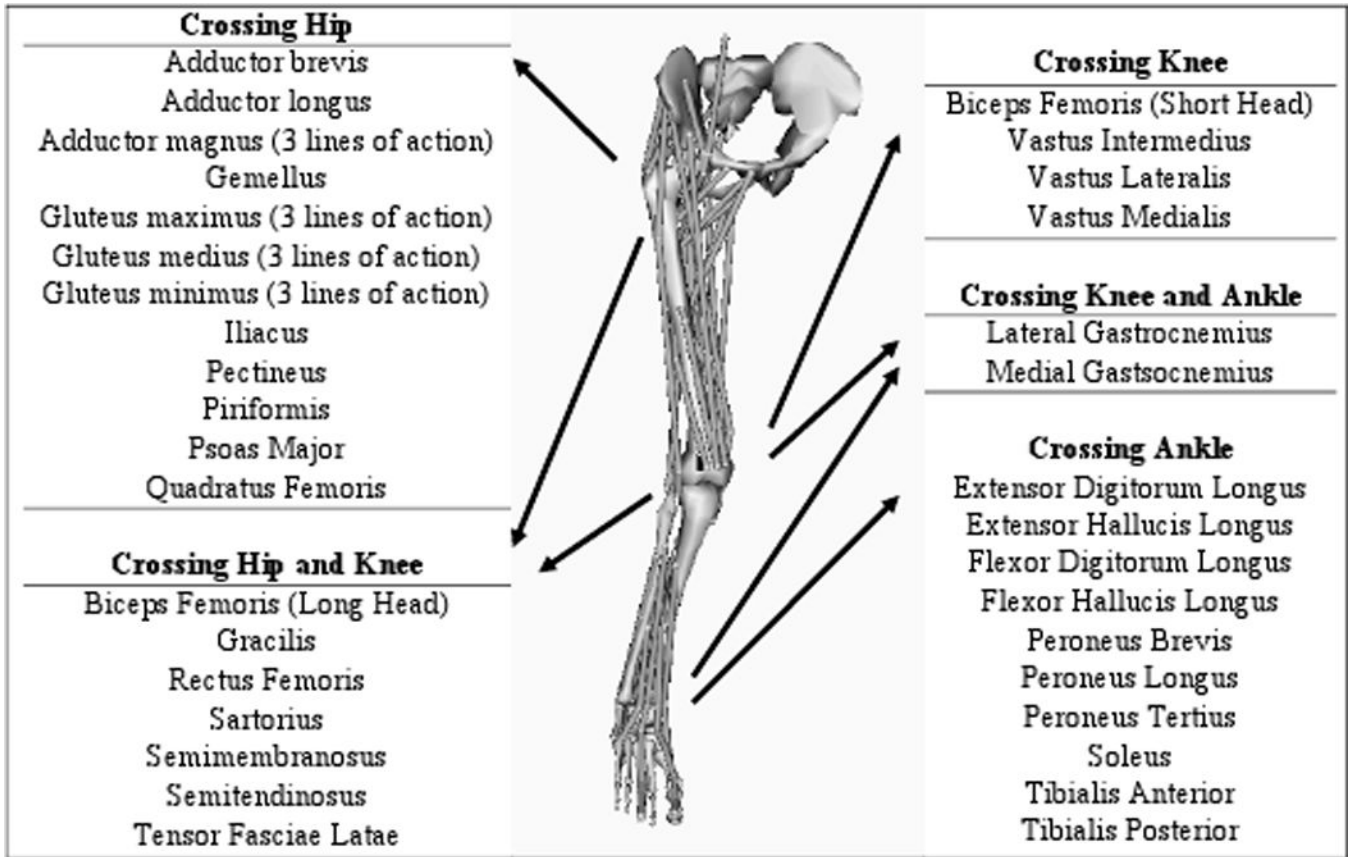


Figure 1. Musculoskeletal model used to estimate muscle forces during gait. The model included 35 muscles crossing the hip, knee and ankle joints as shown.

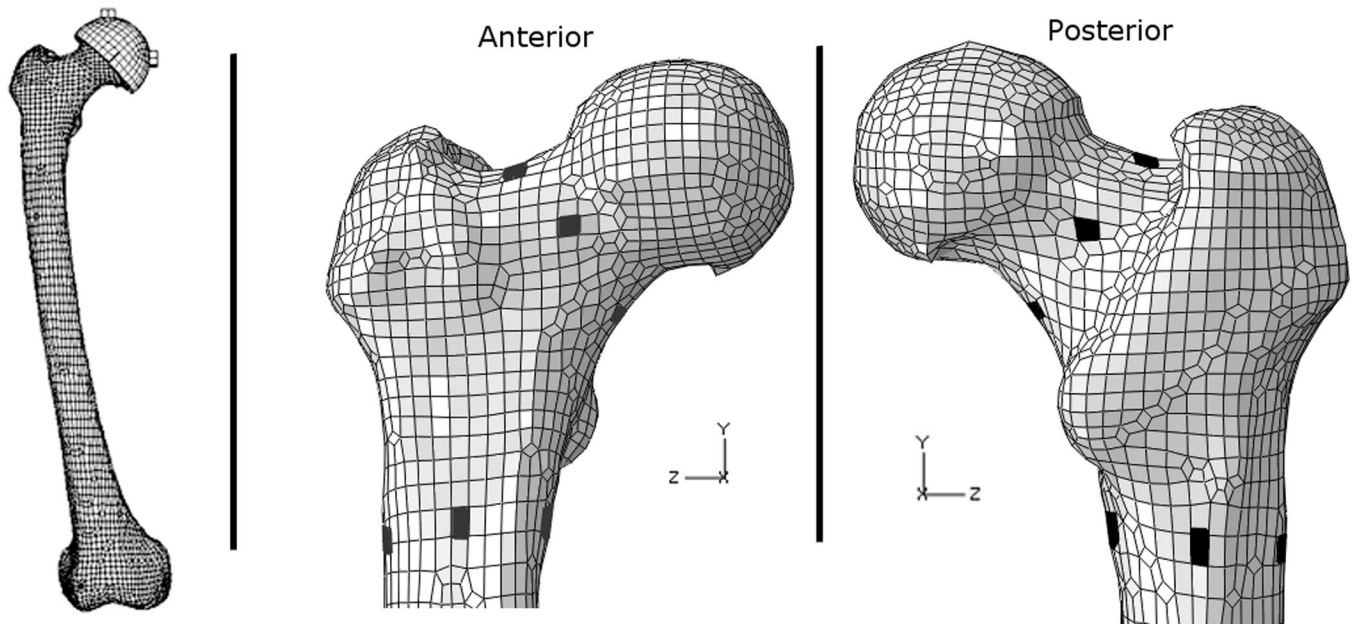


Figure 2. Finite element model of the femur, showing the “acetabulum” part created to apply hip joint loading to the model (left); anterior (center) and posterior (right) views of the proximal portion of the femur finite element mesh. Strains were examined at element centroids of the black elements, four in the femoral neck and four in the sub-trochanteric region.

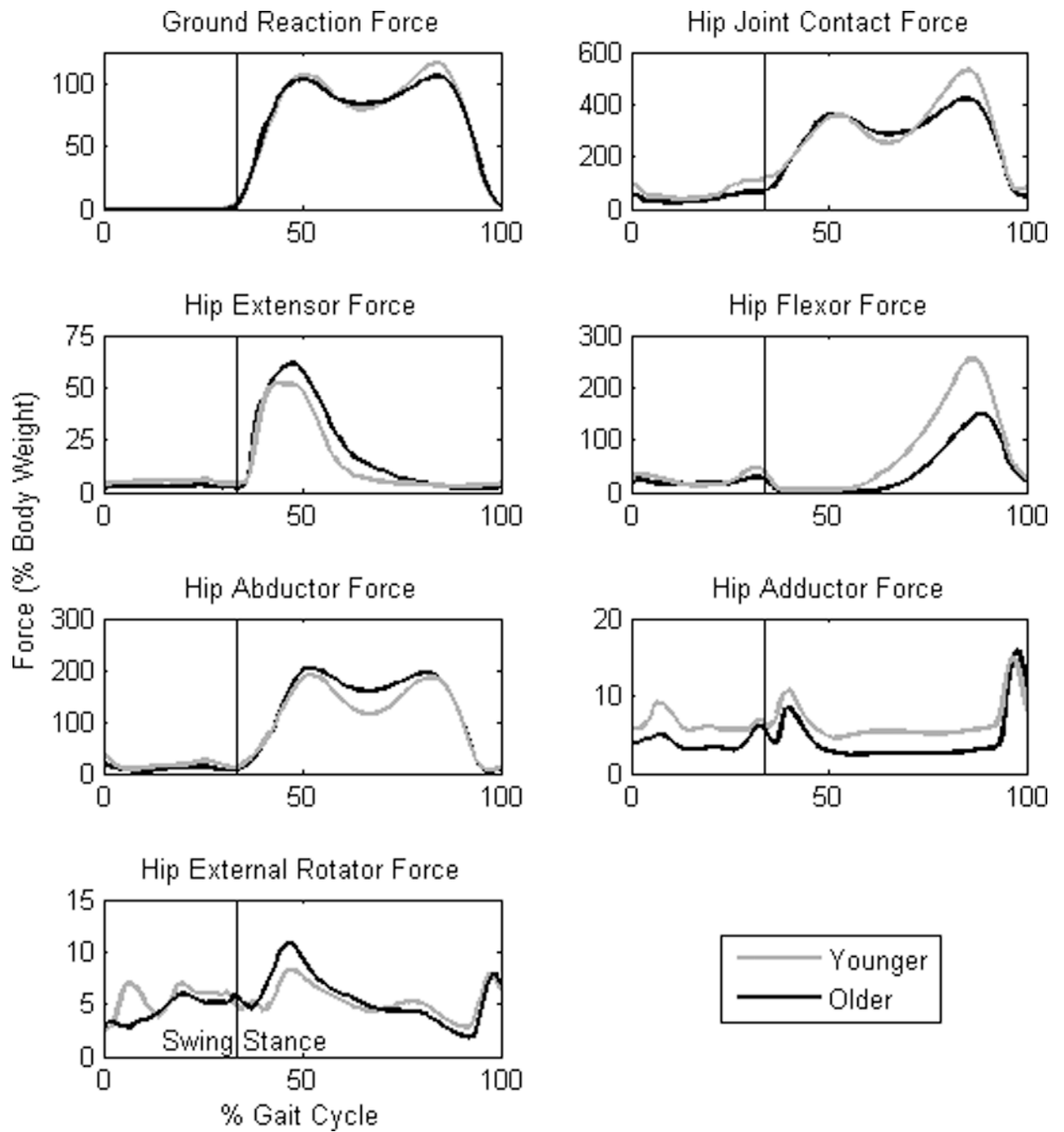


Figure 3. Mean ground reaction forces, hip joint contact forces, and muscle group forces during gait as a percentage of body weight in young and older age groups.

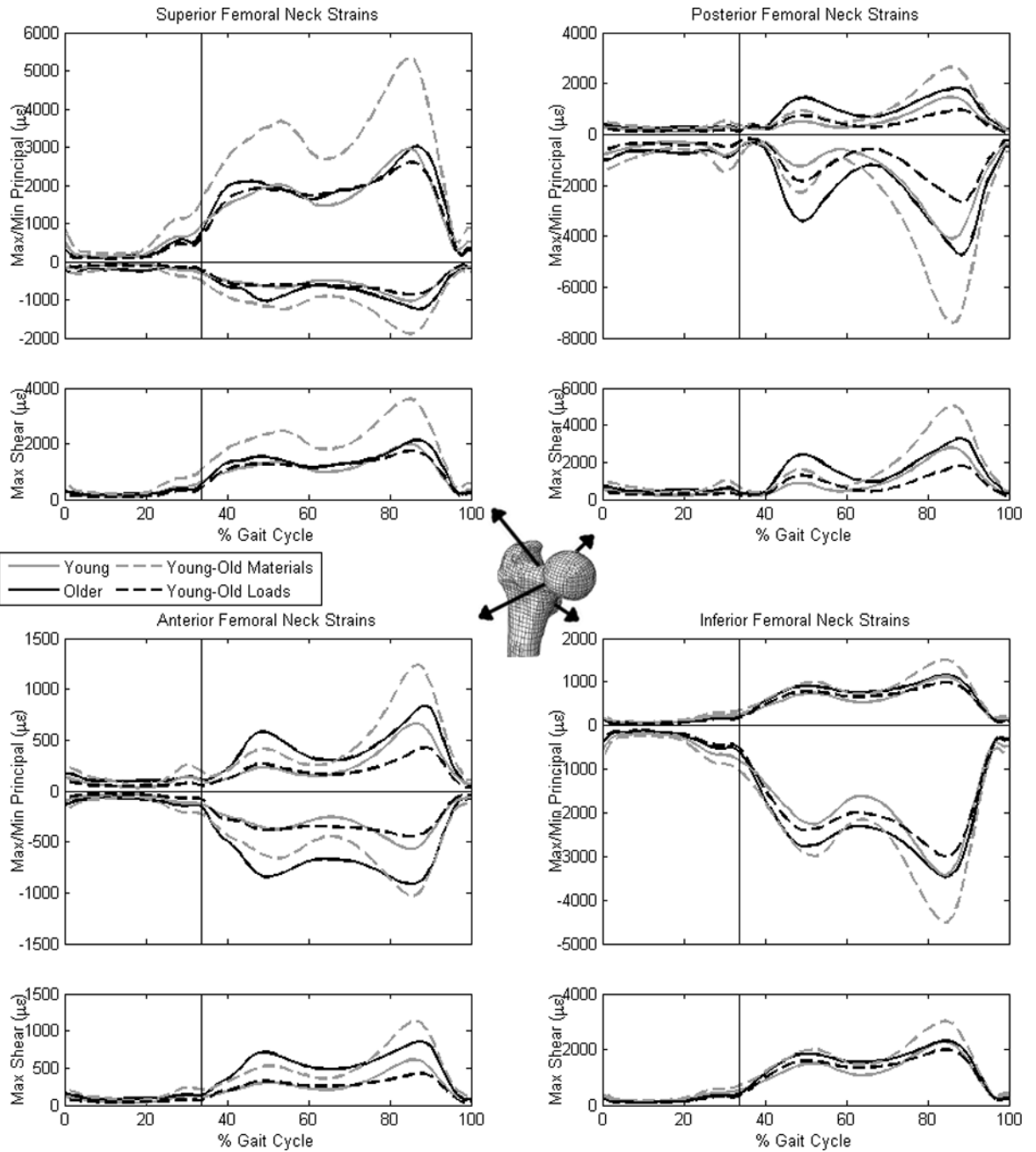


Figure 4. Mean maximum and minimum principal and maximum shear strains in the femoral neck during a full gait cycle from Young, Older, Young-Old Materials and Young-Old Loads models. The vertical lines denote the beginning of stance phase. Note that strain scales are not identical.

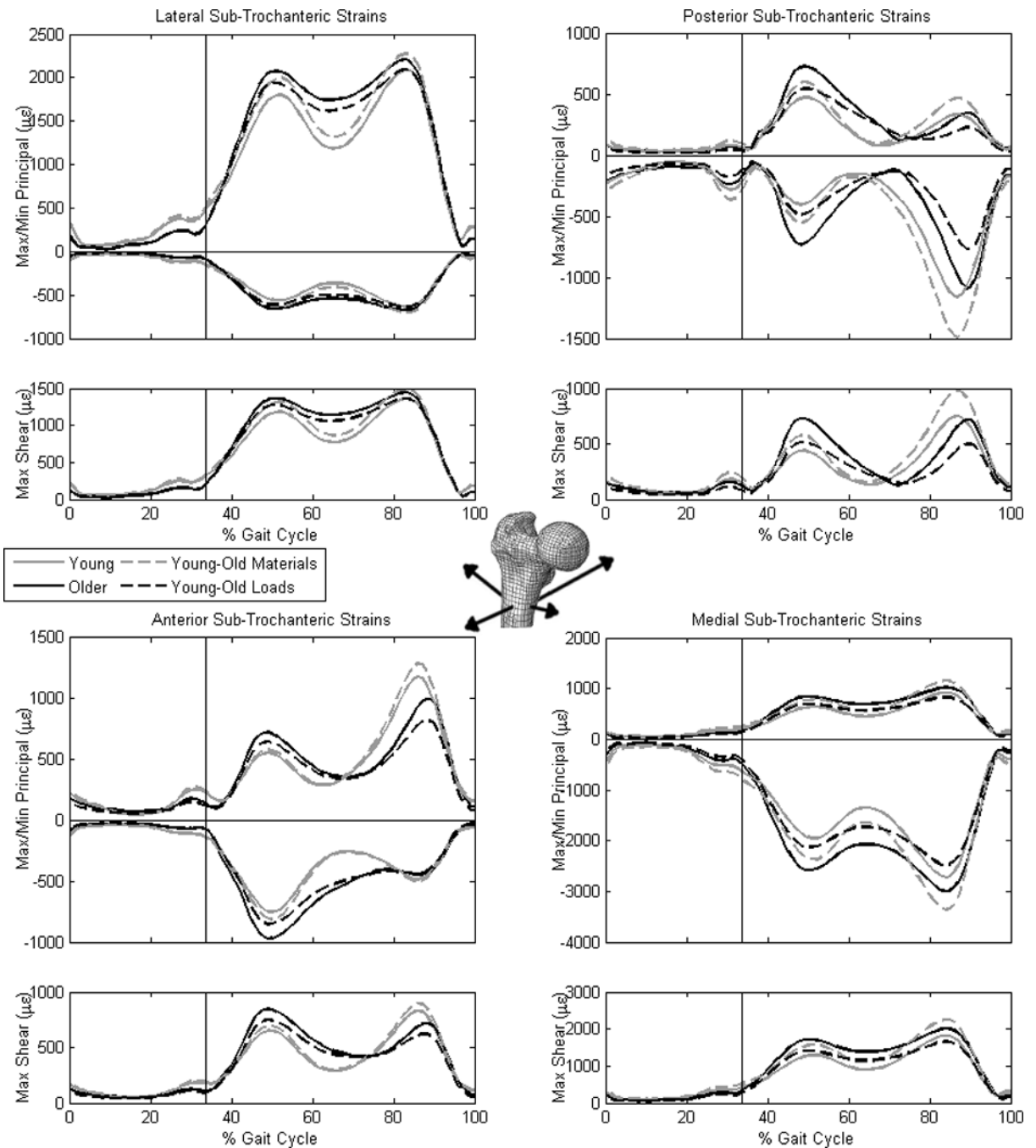


Figure 5. Mean maximum and minimum principal and maximum shear strains in sub-trochanteric locations during a full gait cycle from Young, Older, Young-Old Materials and Young-Old Loads models. The vertical lines denote the beginning of stance phase. Note that strain scales are not identical.

Table 1

Mean (SD) subject characteristics by age group, including femoral characteristics measured from DXA scans.

	Young	Older
Subject Characteristics:		
N [M/F]	5 [2/3]	5 [2/3]
Age (years)	25.0 (4.3)	79.4 (4.6)*
Height (m)	1.66 (0.09)	1.60 (0.05)
Body mass (kg)	64.5 (7.9)	69.0 (5.7)
Femur Characteristics:		
Length (cm)	43.1 (2.1)	42.2 (2.9)
Neck Axis Length (cm)	9.30 (0.71)	9.35 (0.51)
Neck Diameter (cm)	2.93 (0.39)	3.33 (0.28)
Neck Angle (°)	32.4 (3.8)	33.3 (3.1)
Femoral Neck aBMD (g/cm ²)	1.18 (0.25)	0.85 (0.14)*

* Significantly different than young age group ($P < .05$).

Table 2

Mean (SD) of peak forces (% body weight) by age group in early and late stance phase.

Force	Early Stance		Late Stance	
	Young	Older	Young	Older
Ground Reaction	108 (2)	105 (4)	116 (3)	106 (4) *
Hip Joint Contact	363 (28)	368 (26)	529 (55)	428 (63) *
Hip Extensor	54 (11)	64 (10)	-	-
Hip Flexor	-	-	256 (44)	152 (40) *
Hip Abductor	192 (32)	209 (28)	186 (30)	200 (36)
Hip Adductor	13 (7)	10 (3)	16 (7)	17 (4)
Hip External Rotator	9 (3)	12 (5)	9 (2)	8 (2)

* Significantly different than young age group ($P < .05$).

Table 3

Mean (SD) values of peak maximum principal (σ_{max}), minimum principal (σ_{min}) and maximum shear (τ_{max}) strains found in the proximal femur in early stance and late stance.

	Early Stance				Late Stance			
	σ_{max}	σ_{min}	τ_{max}	τ_{min}	σ_{max}	σ_{min}	τ_{max}	τ_{min}
Superior Femoral Neck:								
Young	2075 (233)	-705 (80)	1387 (153)	2953 (598)	-1036 (149)	1994 (367)		
Older	2259 (869)	-1055 (442)	1599 (579)	3027 (2021)	-1262 (577)	2140 (1286)		
Young-Old Materials	3790 (1324)*	-1293 (472)*	2535 (898)*	5330 (1712)*	-1904 (441)*	3615 (1070)*		
Young-Old Loads	2115 (345)	-710 (121)	1411 (232)	2664 (925)	-897 (306)	1780 (614)		
Anterior Femoral Neck:								
Young	242 (85)	-388 (53)	310 (63)	672 (296)	-572 (207)	618 (254)		
Older	593 (241)*	-856 (167)*	722 (193)*	851 (241)	-934 (174)*	870 (195)		
Young-Old Materials	428 (144)*	-679 (120)*	543 (120)*	1254 (426)*	-1035 (318)*	1140 (373)*		
Young-Old Loads	271 (90)	-398 (79)	328 (81)	437 (133)*	-456 (94)	433 (100)		
Inferior Femoral Neck:								
Young	754 (99)	-2303 (306)	1529 (202)	1120 (121)	-3424 (361)	2272 (241)		
Older	924 (188)	-2826 (578)	1875 (383)	1162 (341)	-3519 (1047)	2341 (694)		
Young-Old Materials	1009 (185)*	-3052 (537)*	2031 (361)*	1506 (214)*	-4520 (584)*	3013 (399)*		
Young-Old Loads	798 (131)	-2443 (408)	1621 (270)	1002 (264)	-3049 (801)	2026 (533)		
Posterior Femoral Neck:								
Young	568 (189)	-1461 (485)	1014 (336)	1478 (528)	-4153 (1441)	2814 (985)		
Older	1471 (582)*	-3461 (1611)*	2462 (1098)*	1873 (611)	-4818 (1690)	3338 (1142)		
Young-Old Materials	1031 (246)*	-2620 (655)*	1824 (448)*	2674 (708)*	-7517 (2017)*	5093 (1362)*		
Young-Old Loads	743 (360)	-1868 (970)	1304 (667)	978 (383)*	-2711 (1025)*	1843 (702)*		
Lateral Sub-trochanteric:								
Young	1828 (278)	-571 (93)	1199 (186)	2088 (332)	-636 (102)	1362 (217)		
Older	2112 (429)	-669 (143)	1391 (286)	2288 (745)	-701 (229)	1495 (487)		

	Early Stance			Late Stance		
	max	min	max	max	min	max
Young-Old Materials	2032 (314)*	-644 (108)*	1338 (211)*	2275 (380)*	-705 (118)*	1490 (249)*
Young-Old Loads	1974 (325)	-620 (106)	1297 (215)	2153 (569)	-657 (173)	1405 (370)
Anterior Sub-trochanteric:						
Young	555 (177)	-760 (181)	655 (167)	1192 (299)	-486 (91)	839 (190)
Older	741 (277)	-985 (274)	858 (274)	1003 (327)	-539 (229)	723 (275)
Young-Old Materials	582 (184)*	-820 (189)*	699 (171)*	1305 (332)*	-509 (105)*	906 (215)*
Young-Old Loads	663 (200)	-864 (180)*	760 (189)	833 (171)	-510 (142)	631 (142)
Medial Sub-trochanteric:						
Young	652 (89)	-1987 (272)	1319 (180)	914 (93)	-2723 (279)	1818 (186)
Older	855 (169)*	-2631 (531)*	1743 (350)*	1039 (260)	-3055 (772)	2047 (516)
Young-Old Materials	798 (106)*	-2401 (311)*	1599 (208)*	1153 (150)*	-3355 (427)*	2254 (288)*
Young-Old Loads	708 (123)	-2169 (356)	1439 (240)	846 (205)	-2531 (640)	1689 (422)
Posterior Sub-trochanteric:						
Young	489 (170)	-418 (161)	444 (156)	347 (122)	-1186 (376)	767 (248)
Older	750 (218)*	-744 (296)*	741 (261)*	364 (128)	-1092 (354)	723 (237)
Young-Old Materials	612 (196)*	-569 (205)*	582 (191)*	486 (177)*	-1517 (532)*	1002 (354)*
Young-Old Loads	566 (143)*	-493 (190)	524 (168)	283 (77)	-770 (198)*	503 (120)

Note. Strains presented in micro-strain (μ).

* Significantly different than Young model ($P < .05$).